# Supplementary Material

# A Nitrogen Rich Covalent Triazine Framework as Photocatalyst for Hydrogen Production

Ruizhi Gong[a], Liuliu Yang[a], Shuo Qiu[a], Wan-Ting Chen[b], Qing Wang[b], Jiazhuo Xie[d], Geoffrey I.N. Waterhouse[a,b,c,]*, Jing Xu[a]*

[a]College of Chemistry and Material Science, Shandong Agricultural University, Tai′an, Shandong 271018, PR China

[b]School of Chemical Sciences, The University of Auckland, Auckland, New Zealand.

[c]The MacDiarmid Institute for Advanced Materials and Nanotechnology, New Zealand.

[d]College of Resources and Environment, Shandong Agricultural University, Tai′an, Shandong 271018, PR China

*Corresponding authors:

Prof. Jing Xu

Email: jiaxu@sdau.edu.cn

Telephone number: 86 538 8249248

E-mail: 86 538 8242251

Prof. Geoffrey I.N. Waterhouse

Email: g.waterhouse@auckland.ac.nz

Telephone number: 64-9-9237212

Fax number: 64-9-373 7422

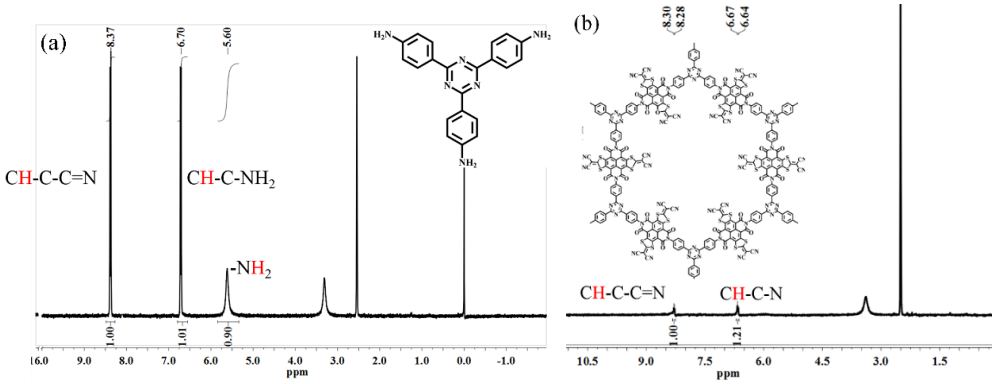


FIGURE S1: $^{1}$H NMR spectra for (a) TAPT and (b) CTF-CN. The samples were dissolved in deuterated DMSO for the analyses.

TAPT has 3 unique proton environments, giving rise to signals with chemical shifts δ = 8.37, 6.70 and 5.60 ppm. These are present in a 1:1:1 area ratio. In the $^{1}$H NMR spectrum of CTF-CN, environments CH-C-C=N (8.30, 8.28 ppm) and CH-C-N (6.67, 6.64 ppm) remain, but environment the –$NH_2$ signal has been lost, confirming the successful incorporation of TAPT into the CTF-CN structure.

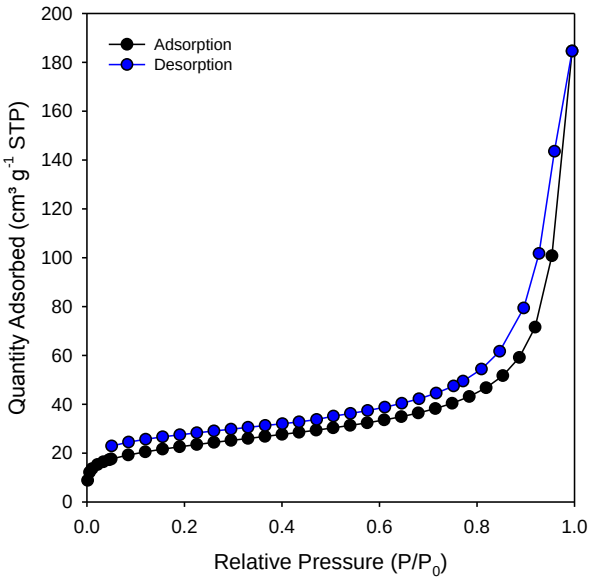


FIGURE S2: $N_2$ adsorption and desorption isotherms for CTF-CN collected at 77 K.

TABLE S1: Summarised XPS chemical composition data for CTF-CN, its precursors and g-$C_3N_4$ reference photocatalyst. Data for Pt/CFT-CN and Pt/g-$C_3N_4$ is also included.

| **Sample** | **Atom %** | | | | | | |
|---|---|---|---|---|---|---|---|
| | **C** | **N** | **O** | **Br** | **Na** | **S** | **Pt** |
| TBNDA | 65.9 | - | 21.2 | 13.0 | - | - | - |
| $Na_2$(i-mnt) | 51.3 | 9.5 | 16.3 | - | 10.3 | 12.6 | - |
| TAPT | 80.2 | 16.2 | 3.5 | - | - | - | - |
| CTF-CN | 76.8 | 8.4 | 10.2 | 0.6 | - | 4.0 | - |
| Pt/CTF-CN | 74.9 | 8.5 | 12.9 | 0.3 | - | 3.3 | 0.1 |
| g-$C_3N_4$ | 47.9 | 49.4 | 2.8 | - | - | - | - |
| Pt/g-$C_3N_4$ | | | | - | - | - | - |

TABLE S2: N 1s peak position for different N environments.

| **N environment** | **Peak position (eV)** |
|---|---|
| pyridinic N | 398.3 |
| amine ($NH_2$) | 399.3 |
| pyridinic NH | 399.7 |
| NC=O | 400.3 |
| graphitic N | 400.9 |
| C-N | 401.3 |
| cyano (C≡N) | 401.9 |
| pyridinic oxide | 402.6 |
| π-π* | 404.0 |

TABLE S3: C 1s peak position for different C environments.

| **C environment** | **Peak position (eV)** |
|---|---|
| C=C/C-C | 284.9 |
| C-N/C≡N/C-S | 286.0 |
| C-Br | 286.6 |
| N=C-N | 288.2 |
| O-C=O | 288.4 |
| π-π* | 290.3 |
| π-π* | 291.4 |

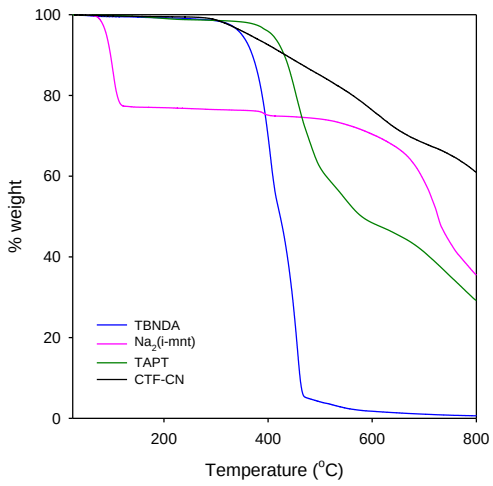


FIGURE S3: TGA data for CTF-CN and the starting materials used in the synthesis of CTF-CN. All data was collected at a heating rate of 10 °C $min^{-1}$ under a $N_2$ atmosphere.

The TGA data shows that CTF-CN is stable up to ~350 °C, confirming that the material has excellent thermal stability.

TABLE S4**:** Summarized $H_2$ production data for Pt/CTF-CN and Pt/g-$C_3N_4$ photocatalysts.

| **Photocatalyst** | **Run #** | **Surface area ($m^2$ $g^{-1}$)** | **$H_2$ production rate (µmol $g^{-1}$ $h^{-1}$)** | **$H_2$ production rate (µmol $m^{-2}$ $h^{-1}$)** |
|---|---|---|---|---|
| Pt/CTF-CN | Run 1 | 96.0 | 484.7 | 5.049 |
| Pt/CTF-CN | Run 2 | 96.0 | 468.4 | 4.879 |
| Pt/CTF-CN | Run 3 | 96.0 | 481.3 | 5.014 |
| Pt/CTF-CN | Run 4 | 96.0 | 479.9 | 5.000 |
| Pt/CTF-CN* | - | 96.0 | 478.6 | 4.985 |
| Pt/g-$C_3N_4$ | - | 108.3 | 1088.8 | 10.054 |

*$H_2$ production data is the mean of runs 1-4.

TABLE S5: Performance comparison of different covalent triazine framework (CTF)-based photocatalysts for $H_2$ production under visible ($\lambda > 420$ nm) or UV-visible irradiation.

| **Catalyst** | **Co-catalyst** | **Sacrificial Agent** | **Solvent** | **Light source** | **$H_2$ rate ($\mu mol\ g^{-1}\ h^{-1}$)** | **Ref** |
|---|---|---|---|---|---|---|
| PCTF-8 | Pt | TEOA | pH 7 PBS | 300 W Xe | 119 | 30 |
| PCTF-8 | Pt | MeOH | pH 7 PBS | 300 W Xe | 89 | 30 |
| CTF-1_10 | Pt | TEOA | $H_2O/CH_3CN$ | 300 W Xe | 1072 | 26 |
| CTF-1_30 | Pt | TEOA | $H_2O/CH_3CN$ | 300 W Xe | 138 | 26 |
| CTF-HUST-1 | Pt | TEOA | Water | 300 W Xe | 1460 | 19 |
| CTF-HUST-2 | Pt | TEOA | Water | 300 W Xe | 2647 | 19 |
| CTF-HUST-3 | Pt | TEOA | Water | 300 W Xe | 1238 | 19 |
| CTF-HUST-4 | Pt | TEOA | Water | 300 W Xe | 1582 | 19 |
| $CTFS_{10}$ | Pt | TEOA | Water | λ>420 nm | 2000 | 35 |
| CTF-T1 | Pt | TEOA/$AgNO_3$ | Water | λ>420 nm | 250 | 25 |
| CTF-T2 | Pt | TEOA/$AgNO_3$ | Water | λ>420 nm | 50 | 25 |
| CdsNPs/3%CTF-1 | Pt | Lactic acid | Water | λ>420 nm | 12150 | 36 |
| CTF-1-100 W | Pt | TEOA/MeOH | Water | 300 W Xe | 360 | 27 |
| CTF-1-100 W | none | TEOA/MeOH | Water | 300 W Xe | 5 | 27 |
| 2wt%Pt/CTF-1-100 W | Pt | TEOA/MeOH | Water | 300 W Xe | 5500 | 27 |
| CTF-CN | Pt | TEOA/MeOH | Water | 300 W Xe | 480 | This work |

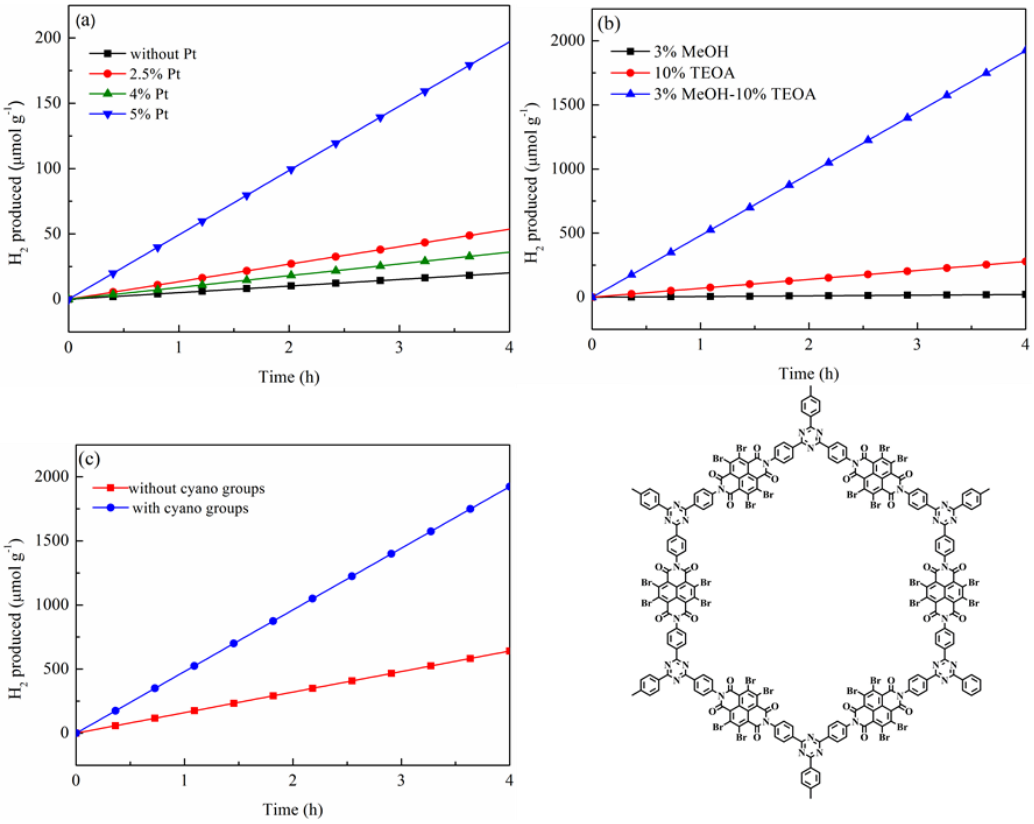


FIGURE S4: (a) $H_2$ production data for CTF-CN with different co-catalyst Pt content, (b) $H_2$ production data for CTF-CN with different sacrifices, and (c) $H_2$ production data for CTF-CN and CTF(without cyano groups).

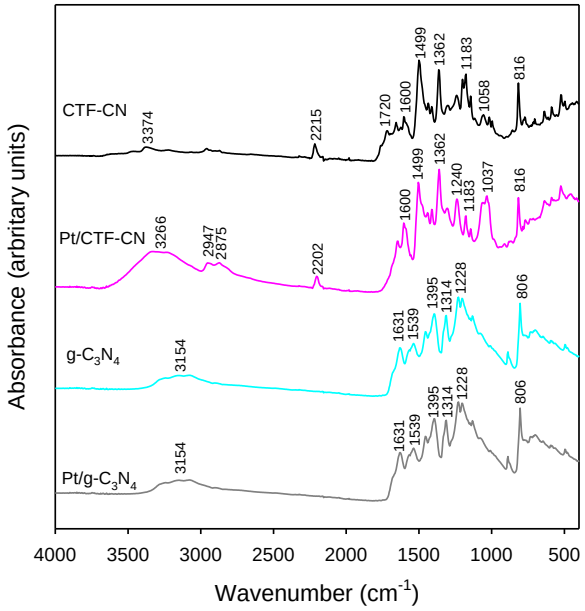

FIGURE S5: FT-IR absorbance spectra for CTF-CN and g-$C_3N_4$ before and after the $H_2$ production tests. During the $H_2$ production tests, aqueous Pt(II) was photoreduced to $Pt^0$ on the surface of the photocatalyst.

TABLE S6: Summarized $H_2$ production data for various Pt/g-$C_3N_4$ photocatalysts

| Catalyst | Pt (wt.. %) | $H_2$ rate ($\mu$mol $g_{Catal}^{-1}$ $h^{-1}$) | Sacrificial agent | Wavelength nm | Lamp power/Flux | **ref** |
|---|---|---|---|---|---|---|
| g-$C_3N_4$/$Cu_2O$ | 3 | 241 | TEOA, 10 vol.% | >420 | Xe 300W/not given | 16 |
| g-$C_3N_4$/$In_2O_3$ | 0.5 | 1 | ascorbic acid 0.1 M | >420 | Xe 300W/200mWcm$^{-2}$ | 13 |
| g-$C_3N_4$ | 3 | 3300 | TEOA, 10 vol.% | >395 | Xe 300W/not given | 6 |
| g-$C_3N_4$/$TiO_2$ | 1 | ca.330[a] | TEOA, 10 vol.% | >400 | Xe 300W/not given | 4 |
| g-$C_3N_4$/CdS | 0.5 | 4500[b] (2500)[c] | ascorbic acid 0.1 M | >420 | Xe 300W/not given QY = 8% | 14 |
| g-$C_3N_4$/Zn | 0.5 | 60 | methanol, 25 vol.% | >420 | Xe 200W QY = 3.2% at 420nm and 0.8mW/cm$^2$ | 12 |
| g-$C_3N_4$/$MoS_2$ | 1 | 230[d] | methanol, 25 vol.% | >400 | Xe 300W QY = 2.8% | 15 |
| g-$C_3N_4$ | 3 | 140 | TEOA, 10 vol.% | >420 | Hg 500W/not given | 2 |
| g-$C_3N_4$ | 3 | 100 | TEOA, 10 vol.% | >420 | Xe 300W QY=0.1% (420-460nm) | 1 |
| g-$C_3N_4$ | 3 | 470[e] | TEOA, 10 vol.% | >400 | Xe 300W/solar filter | 3 |
| g-$C_3N_4$/CQD[f] | 0 | 575[g] | none | >420 | Xe 300W/ QY = 16% (410-430 nm) | 7 |

a. Rate based on a 3 h reaction period

b. Hydrogen production is not linear (decreases with time).

c. Hydrogen production rate over hybrid

d. Hydrogen production rate decreased with time

e. BET surface area = 70 m$^2$/g

f. Carbon quantum dots

g. BET surface area = 93 $m^2/g$

h. BET surface area = 10 $m^2/g$

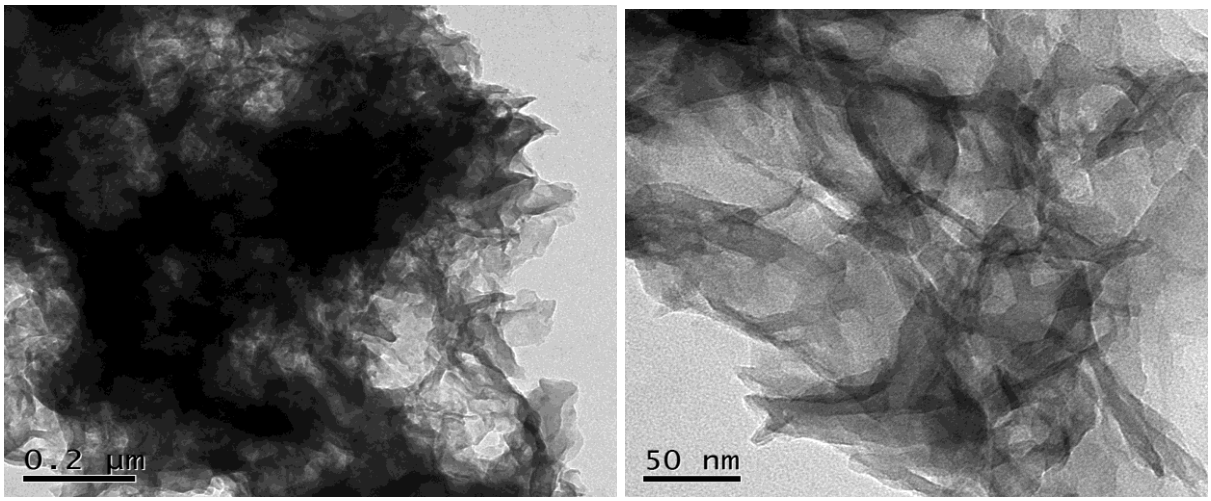


FIGURE S6: TEM images of CTF-CN synthesized using the microwave method